

1  
2  
3  
4  
5  
6  
7  
8  
9  
10  
11  
12  
13  
14  
15  
16

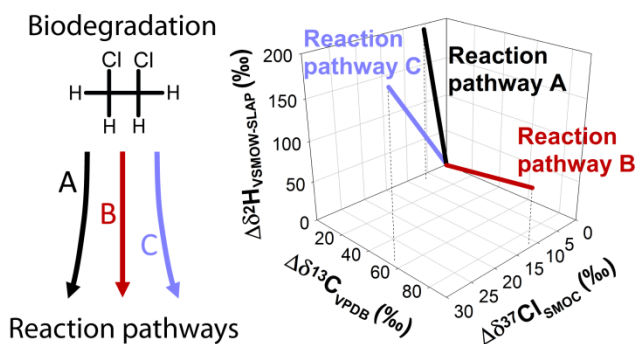
This document is the unedited Author's version of a Submitted Work that was subsequently accepted for publication in *Environmental Science and Technology*, copyright © American Chemical Society after peer review. To access the final edited and published work see:

<http://pubs.acs.org/articlesonrequest/AOR-Zy933XtE4s53i7UpARj2>



41 **ABSTRACT**

42 Even though multi-element isotope fractionation patterns provide crucial information to  
43 identify contaminant degradation pathways in the field, those involving hydrogen are still  
44 lacking for many halogenated groundwater contaminants and degradation pathways. This  
45 study investigates for the first time hydrogen isotope fractionation during both aerobic and  
46 anaerobic biodegradation of 1,2-dichloroethane (1,2-DCA) using five microbial cultures.  
47 Transformation-associated isotope fractionation values ( $\epsilon_{\text{bulk}}^{\text{H}}$ ) were:  $-115 \pm 18\text{‰}$  (aerobic  
48 C-H bond oxidation),  $-34 \pm 4\text{‰}$  and  $-38 \pm 4\text{‰}$  (aerobic C-Cl bond cleavage via hydrolytic  
49 dehalogenation),  $-57 \pm 3\text{‰}$  and  $-77 \pm 9\text{‰}$  (anaerobic C-Cl bond cleavage via reductive  
50 dihaloelimination). The dual element C-H isotope approach ( $\Lambda_{\text{C-H}} = \Delta\delta^2\text{H}/\Delta\delta^{13}\text{C} \approx$   
51  $\epsilon_{\text{bulk}}^{\text{H}}/\epsilon_{\text{bulk}}^{\text{C}}$ , where  $\Delta\delta^2\text{H}$  and  $\Delta\delta^{13}\text{C}$  are changes in isotope ratios during degradation)  
52 resulted in clearly different  $\Lambda_{\text{C-H}}$  values:  $28 \pm 4$  (oxidation),  $0.7 \pm 0.1$  and  $0.9 \pm 0.1$   
53 (hydrolytic dehalogenation),  $1.76 \pm 0.05$  and  $3.5 \pm 0.1$  (dihaloelimination). This result  
54 highlights the potential of this approach to identify 1,2-DCA degradation pathways in the  
55 field. In addition, distinct trends were also observed in a multi (i.e.,  $\Delta\delta^2\text{H}$  vs  $\Delta\delta^{37}\text{Cl}$  vs  
56  $\Delta\delta^{13}\text{C}$ ) isotope plot, which opens further possibilities for pathway identification in future  
57 field studies. This is crucial information to understand the mechanisms controlling natural  
58 attenuation of 1,2-DCA and to design appropriate strategies to enhance biodegradation.



59

TOC Art

## 60 INTRODUCTION

61 1,2-dichloroethane (1,2-DCA) is widely used as a chemical intermediate in the industrial  
62 production of polyvinyl chloride, as a solvent and also as a lead scavenger in leaded  
63 gasoline.<sup>1</sup> Due to its high production, accidental leakage and improper disposal, 1,2-DCA  
64 has become a prevalent groundwater contaminant. For instance, in 2015 a total of 186 tons  
65 of 1,2-DCA (not including on-site land disposal) were released to the environment in the  
66 U.S.,<sup>2</sup> which poses a threat to human and wildlife health due to its high toxicity.<sup>3</sup>

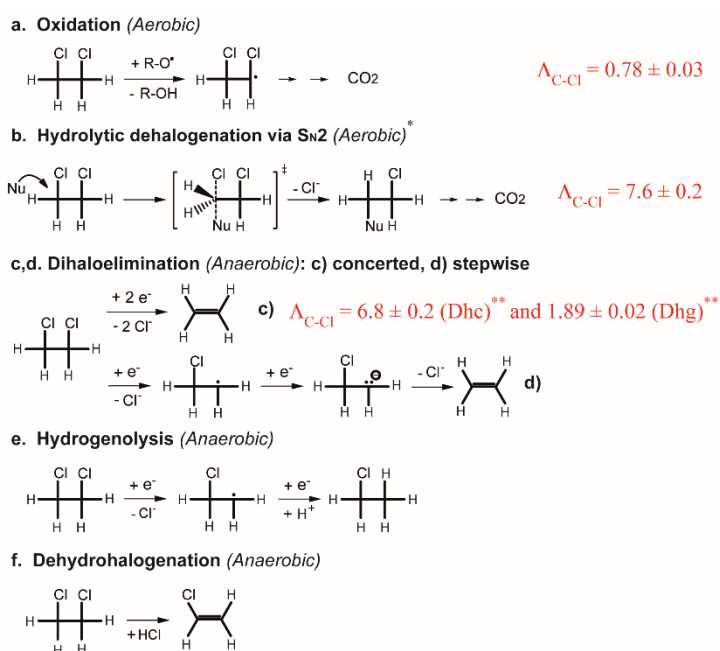
67 1,2-DCA can undergo biodegradation via distinct degradation pathways under oxic<sup>4-6</sup>  
68 and anoxic conditions<sup>7-11</sup> (Scheme 1). Under oxic conditions, 1,2-DCA can be biodegraded  
69 by oxidation via a monooxygenase<sup>4</sup> (Scheme 1a) and hydrolytic dehalogenation<sup>5, 6</sup>  
70 (Scheme 1b). Initial products of both reactions are further degraded to innocuous end  
71 products. Under reducing conditions, 1,2-DCA is usually transformed by dihaloelimination  
72 to ethene<sup>7, 8</sup> (either concerted or stepwise  $\beta$ -elimination, Scheme 1c, d) or hydrogenolysis  
73 to chloroethane (CA)<sup>11</sup> (Scheme 1e). In addition, 1,2-DCA can be transformed to vinyl  
74 chloride (VC) via dehydrohalogenation (Scheme 1f) by pure *Dehalococcoides* strains<sup>12, 13</sup>  
75 and *Dehalococcoides*-containing cultures,<sup>10, 14</sup> however, VC is typically detected at much  
76 lower concentrations compared to ethene. Therefore, chlorinated products such as CA and  
77 VC can accumulate under anoxic conditions. Like 1,2-DCA, both CA and VC are  
78 groundwater contaminants and are considered as priority pollutants by the U.S.  
79 Environmental Protection Agency (USEPA),<sup>3</sup> emphasizing the need for elucidation of  
80 active biodegradation pathways in the field.

81 Owing to the high susceptibility for 1,2-DCA to be transformed under different redox  
82 conditions, the assessment of its fate in the subsurface is not an easy task. On the one hand,  
83 aerobic biodegradation of 1,2-DCA might be sustained at very low dissolved oxygen  
84 concentrations as shown for VC oxidation.<sup>15</sup> Furthermore, anaerobic oxidation of 1,2-DCA

85 was demonstrated under nitrate-reducing conditions,<sup>16, 17</sup> likely via hydrolytic  
 86 dehalogenation (Scheme 1b).<sup>18</sup> On the other hand, contaminated sites are usually impacted  
 87 by mixtures of compounds, which complicates pathway identification from analysis of  
 88 degradation products because the same products can be formed from different precursors.  
 89 For instance, CA can also be formed from 1,1,1-trichloroethane (1,1,1-TCA)<sup>19</sup> and VC and  
 90 ethene from trichloroethene (TCE)<sup>12</sup> by reductive dechlorination. In addition, end products  
 91 of the aerobic degradation pathways of 1,2-DCA, i.e., inorganic carbon and Cl<sup>-</sup>, are  
 92 ubiquitous and often occur at high background concentrations in groundwater. Hence,  
 93 additional tools are necessary for better characterization of 1,2-DCA biodegradation in the  
 94 field. This information is essential for i) evaluating the natural attenuation of 1,2-DCA at  
 95 contaminated sites; and ii) predicting potential accumulation of toxic products.

96

97 **Scheme 1.** Biodegradation pathways of 1,2-DCA in aqueous systems and reported  $\Lambda_{C-Cl}$   
 98 values.<sup>14</sup> (\*) Transformation via hydrolytic dehalogenation was also proposed under  
 99 nitrate-reducing conditions.<sup>18</sup> (\*\*) Values obtained from experiments with  
 100 *Dehalococcoides-* (Dhc) and *Dehalogenimonas-* (Dhg) containing enrichment cultures.<sup>14</sup>



101

102 Dual carbon and chlorine isotope analysis during substrate transformation is  
103 increasingly used to elucidate biodegradation pathways and obtain insight into enzymatic  
104 reaction mechanisms for chlorinated ethenes<sup>20-23</sup> and ethanes.<sup>14, 24</sup> However, until recently,  
105 a multi-element isotope approach including hydrogen isotope data was not feasible because  
106 on-line hydrogen isotope analysis of chlorinated compounds was hampered by the  
107 formation of HCl during the high-temperature conversion of chlorinated analytes to H<sub>2</sub>.<sup>25</sup>  
108 New analytical methods for on-line compound-specific hydrogen isotope analysis (H-  
109 CSIA) by gas chromatography - isotope ratio mass spectrometry (GC-IRMS) were  
110 developed which largely circumvent the formation of HCl by the use of a chromium metal  
111 reactor interface to form H<sub>2</sub>. These new methods were validated using different compounds  
112 such as chlorinated ethenes and hexachlorocyclohexane.<sup>26-29</sup> For instance,  $\delta^2\text{H}$  values with  
113 a precision better than  $\pm 7\%$  were obtained for both trichloroethene and *cis*-1,2-  
114 dichloroethene (*cis*-DCE) by Shouakar-Stash and Drimmie.<sup>26</sup> H-CSIA studies have so far  
115 been applied to only a few chlorinated compounds<sup>30-32</sup> and, to the best of our knowledge,  
116 multi-element isotope studies including hydrogen isotope data are currently nonexistent for  
117 chlorinated ethanes.

118 Combined shifts in isotope ratios of two elements (e.g.,  $\Delta\delta^2\text{H}$  vs.  $\Delta\delta^{13}\text{C}$ ) generally  
119 exhibit a linear relationship with a slope ( $\Lambda_{\text{C-H}} = \Delta\delta^2\text{H}/\Delta\delta^{13}\text{C}$ ) reflecting the extent of H  
120 and C isotope effects, which are controlled by chemical bond breakage or formation.  
121 Therefore, different  $\Lambda_{\text{C-H}}$  values may be expected for distinct transformation mechanisms  
122 involving different elements.<sup>33</sup> For 1,2-DCA, dual C-Cl isotope data were recently reported  
123 and different  $\Lambda_{\text{C-Cl}}$  values (Scheme 1) were observed during both aerobic<sup>24</sup> and anaerobic<sup>14</sup>  
124 biodegradation of 1,2-DCA. However, relatively similar  $\Lambda_{\text{C-Cl}}$  values were observed for  
125 aerobic hydrolytic dehalogenation by *Xanthobacter autotrophicus* GJ10 and *Ancylobacter*  
126 *aquaticus* AD20 ( $7.6 \pm 0.2$ ) and anaerobic dihaloelimination by a *Dehalococcoides*-

127 containing enrichment culture ( $6.8 \pm 0.2$ ). Taking into account the uncertainty of  
128 measurements at contaminated sites, it may be difficult to distinguish the two pathways  
129 (i.e., hydrolytic dehalogenation vs. dihaloelimination) in field studies solely based on dual  
130 C-Cl isotope data. In addition to C and Cl, analysis of H isotope ratios for 1,2-DCA may  
131 increase the possibilities for a dual- (C vs. H or Cl vs. H) or multi-element (C vs. Cl vs. H)  
132 isotope approach for differentiating between hydrolytic dehalogenation and  
133 dihaloelimination pathways.

134 For dihaloelimination of 1,2-DCA, distinct  $\Lambda_{\text{C-Cl}}$  values were reported from microcosm  
135 experiments with *Dehalococcoides* ( $6.8 \pm 0.2$ ) and *Dehalogenimonas* ( $1.89 \pm 0.02$ )  
136 containing enrichment cultures and a different mode of *concerted* bond cleavage rather  
137 than two different reaction mechanisms (i.e., *stepwise* vs *concerted*) was proposed to  
138 explain this difference.<sup>14</sup> However, further insight into the reductive dehalogenation  
139 mechanisms of 1,2-DCA may be obtained from hydrogen isotope data. Owing to the  
140 usually large hydrogen isotope fractionation ( $\epsilon_{\text{bulk}}^{\text{H}}$ ), secondary hydrogen isotope effects  
141 during C-Cl bond breakage might be detected and measured.<sup>34</sup> In this case, the magnitude  
142 of secondary  $\epsilon_{\text{bulk}}^{\text{H}}$  values may vary depending on the reaction mechanism (i.e., *stepwise* vs  
143 *concerted* dehalogenation).

144 In this study, hydrogen isotope fractionation during biodegradation of 1,2-DCA via  
145 aerobic (oxidation and hydrolytic dehalogenation) and anaerobic (dihaloelimination)  
146 degradation pathways was determined for the first time using different pure microbial  
147 strains and enrichment cultures in laboratory experiments. 2D (H vs. C and H vs. Cl) and  
148 3D (H vs. C vs. Cl) multi-element isotope approaches were used i) to characterize the  $\Lambda_{\text{C-H}}$   
149 and  $\Lambda_{\text{Cl-H}}$  values during biodegradation of 1,2-DCA under different redox conditions; ii) to  
150 determine whether the resultant multi-element isotope patterns are sufficiently different to  
151 distinguish between different pathways, particularly between hydrolytic dehalogenation

152 and dihaloelimination pathways; and iii) to obtain further insight into underlying reaction  
153 mechanisms. In addition, for the 3D isotope approach, new procedures were proposed to  
154 characterize pathway-specific multi-element (Cl, C, H) isotope trends, which can be  
155 applicable to other multi-element isotope studies with three elements.

156

## 157 **MATERIALS AND METHODS**

### 158 **Pure and enrichment cultures**

159 Three pure strains with known initial biotransformation mechanisms were used for the  
160 aerobic experiments: *Pseudomonas* sp. strain DCA1 (oxidation)<sup>4</sup> and *Xanthobacter*  
161 *autotrophicus* GJ10 and *Ancylobacter aquaticus* AD20 (hydrolytic dehalogenation)<sup>5, 6</sup>.  
162 *Pseudomonas* sp. strain DCA1 was kindly provided by E. Edwards (Department of  
163 Chemical Engineering and Applied Chemistry, University of Toronto, Toronto, ON) and *X.*  
164 *autotrophicus* GJ10 (DSMZ 3874) and *A. aquaticus* AD20 (DSMZ 9000) were purchased  
165 (DSMZ, Braunschweig, Germany). The growth medium was prepared as described by  
166 Hunkeler and Aravena<sup>35</sup> and further cultivation details are available in Palau *et al.*<sup>24</sup>

167 Anaerobic cultures for reductive dihaloelimination experiments were prepared using  
168 two enrichment cultures with different bacterial populations, which were characterized in  
169 previous studies to determine organohalide-respiring bacteria (ORB) capable of 1,2-DCA  
170 degradation.<sup>10, 14, 36</sup> The growth media used and cultivation details for *Dehalococcoides* and  
171 *Dehalogenimonas*-containing cultures are available in Palau *et al.*<sup>14</sup>

### 172 **Batch experiments preparation and sampling**

173 Aerobic biodegradation experiments were performed at the University of Neuchâtel (UN),  
174 Switzerland. Microcosm batch tests were prepared in 250 mL glass bottles, which  
175 contained 185 mL of medium and were capped with Mininert™ valves (VICI Precision  
176 Sampling, Baton Rouge, LA). Experiments and controls were amended with 22.5 µL of

177 pure 1,2-DCA to produce an initial aqueous concentration of 1.5 mM (when taking into  
178 account partitioning between the headspace and liquid using Henry's Law). All  
179 experiments were conducted in triplicate. Bottles were shaken upside down to prevent  
180 leakage of the gas phase through the valve. For concentration and isotopic analysis,  
181 aqueous samples (1.5 mL) were taken from the 250 mL bottles at selected time points and  
182 preserved frozen<sup>37</sup> in 2 mL vials with NaN<sub>3</sub> (1 g/L). Abiotic control bottles were prepared  
183 with 185 mL of autoclaved mineral medium and samples were collected and preserved as  
184 described for the experimental bottles.

185 Anaerobic biodegradation experiments with *Dehalococcoides* and *Dehalogenimonas*-  
186 containing cultures were performed at Clemson University (CU), US, and at the  
187 Universitat Autònoma de Barcelona (UAB), Spain, respectively. Microcosms were  
188 prepared in anoxic chambers and the bottles (120 mL total volume) were sealed with  
189 Teflon-faced rubber septa and aluminum crimp caps to maintain anoxic conditions.

190 For the batch tests with *Dehalococcoides*-containing culture, a total of 30 serum bottles  
191 were prepared by dispensing 75 mL of the enrichment culture. 1,2-DCA was added as a  
192 water saturated solution (225 µL per bottle) to produce an initial aqueous phase  
193 concentration of ~0.25 mM. Sodium lactate was added to ensure an excess of electron  
194 equivalents for dechlorination (150 µL of a sodium lactate stock solution containing 456.2  
195 g/L of 60% sodium lactate syrup).<sup>10</sup> Killed controls were prepared by adding phosphoric  
196 acid to the bottles, followed by the 1,2-DCA.

197 For the experiments with *Dehalogenimonas*-containing culture, a total of 16 serum  
198 bottles were prepared by dispensing 65 mL of a sterilized anoxic medium described  
199 elsewhere;<sup>36</sup> however, in half of the bottles pyruvate (5 mM) was replaced by acetate (5  
200 mM) as carbon source. The microcosms were inoculated with 3 mL of the  
201 *Dehalogenimonas*-containing culture and 1,2-DCA was added from a stock solution in

202 acetone to give an initial aqueous phase concentration of ~0.1 mM. Abiotic control bottles  
203 containing the growth medium with 1,2-DCA but without inoculum were prepared as  
204 described for the experimental bottles. In addition, live controls without 1,2-DCA were  
205 prepared to account for the transfer of compounds from previous degradation experiments  
206 with the inoculum.

### 207 **Isotopic and concentration analysis**

208 A detailed description of analytical methods and equipment used for the isotopic and  
209 concentration analysis is available in supporting information (SI). On-line H-CSIA of 1,2-  
210 DCA was performed at Isotope Tracer Technologies Inc., Canada, according to Shouakar-  
211 Stash and Drimmie.<sup>26</sup> Briefly, measurements of hydrogen isotope ratios for 1,2-DCA at  
212 natural abundance were determined by GC-IRMS equipped with a chromium reduction  
213 system. The instrument was tuned and the  $H_3^+$  factor was determined every day before  
214 analysis of standards and samples. The  $H_3^+$  factor usually ranged between 4.5 and 5.5.  
215 Isotope ratios were reported using the  $\delta$ -notation (eq. 1):

216

$$217 \quad \delta^2H_{\text{sample}} = \frac{R_{\text{sample}}}{R_{\text{standard}}} - 1 \quad (1)$$

218

219 where  $R = {}^2H/{}^1H$ , corresponding to the ratio of  $m/z$  3 ( ${}^2H{}^1H$ ) to  $m/z$  2 ( ${}^1H{}^1H$ ) measured in  
220 separate Faraday caps. The  $\delta$ -values were expressed in per mil (1 ‰ = 1 mUr) and the  
221 notations  $\delta^2H_{\text{VSMOW-SLAP}}$  and  $\Delta\delta^2H_{\text{VSMOW-SLAP}}$  were used to indicate calibrated  $\delta$ -values and  
222 changes in calibrated  $\delta$ -values during degradation (i.e.,  $\Delta\delta^2H = \delta^2H_t - \delta^2H_0$ ), respectively.  
223 Hydrogen isotope ratios were calibrated using 1,2-DCA and TCE as reference compounds  
224 in the  $\delta^2H_{\text{VSMOW-SLAP}}$ -range between  $-50 \pm 1\text{‰}$  to  $+565 \pm 4\text{‰}$ .<sup>27, 38</sup> External laboratory  
225 standards of 1,2-DCA and TCE were dissolved in water and measured similarly to the  
226 samples. Further details about  $\delta^2H$  values (two-point) calibration to the VSMOW-SLAP

227 scale are available in the SI. Additional aqueous standards of 1,2-DCA were interspersed in  
228 each sample sequence to ensure stability of the measurements during the course of sample  
229 analyses. Samples and standards were diluted to a similar concentration and measured in  
230 duplicate. Precision ( $1\sigma$ ) of the  $\delta^2\text{H}$  values for 1,2-DCA on the analysis of the standards  
231 was  $< 5\text{‰}$  ( $n=54$ ) (see further details in SI).

232 The concentrations of 1,2-DCA were measured by headspace analysis using a GC -  
233 mass spectrometer (GC-MS) at UN<sup>24</sup> laboratory (aerobic experiments) and a GC - flame  
234 ionization detector (GC-FID) at the CU<sup>10</sup> and UAB<sup>36</sup> laboratories (anaerobic experiments).  
235 The concentration of 1,2-DCA in the abiotic controls for the aerobic ( $1.55 \pm 0.03$  mM,  $n =$   
236  $12$ ) and anaerobic experiments ( $0.257 \pm 0.004$  mM,  $n = 5$  and  $0.094 \pm 0.009$  mM,  $n = 6$ )  
237 remained at the initial concentration during the experiments, indicating that compound  
238 losses through the caps and abiotic degradation during incubation were insignificant.

### 239 **Evaluation of isotope fractionation**

240 For a given substrate, the relationship between observable compound-average isotope  
241 fractionation ( $\epsilon_{\text{bulk}}$ ) and the extent of biotransformation can be described by a modified  
242 form of the Rayleigh distillation equation (2) in laboratory experiments:

243

$$244 \ln \frac{R_t}{R_0} = \ln \left( \frac{1 + \delta^2\text{H}_t}{1 + \delta^2\text{H}_0} \right) = \epsilon_{\text{bulk}}^{\text{H}} \cdot \ln f \quad (2)$$

245

246 where the subscripts “t” and “0” refer to the current and initial bulk isotope ratios,  
247 respectively, and  $f$  is the remaining fraction of the substrate.

248 For the aerobic experiments,  $f$  was corrected for substrate removal by repetitive liquid  
249 samples withdrawn from the same batch reactor according to Buchner *et al.* (see SI, eq. S1  
250 and eq. S2),<sup>39</sup> which also takes into account volatilization of the substrate to the bottle  
251 headspace. An aqueous phase 1,2-DCA concentration decrease of  $< 5\%$  was estimated as a

252 result of the change in the headspace to solution ratio during the aerobic experiments. The  
253 correction of  $f$  due to mass removal during sampling was not necessary for the anaerobic  
254 experiments because these were prepared with numerous parallel replicates, which were  
255 sequentially sacrificed for sampling.

256  $\epsilon_{\text{bulk}}$  values were quantified by least squares linear regression of eq. 2 without forcing  
257 the regression through the origin (see SI, Figure S1).<sup>40</sup> Uncertainties are represented by  
258 95% confidence intervals (C.I.). Calculation of position-specific apparent kinetic isotope  
259 effects (AKIEs) is indicated in the SI.

260 Dual-element isotope fractionation patterns for different degradation pathways were  
261 characterized by the slope of the linear regressions in a 2D isotope plot, i.e.,  $\Lambda_{\text{C-H}} =$   
262  $\Delta\delta^2\text{H}/\Delta\delta^{13}\text{C}$  and  $\Lambda_{\text{Cl-H}} = \Delta\delta^2\text{H}/\Delta\delta^{37}\text{Cl}$ ,  $\pm$  95% C.I. For each degradation experiment, the  
263 observed multi-element (Cl, C, H) isotope fractionation trend in a 3D isotope plot was  
264 characterized by principal component analysis in SigmaPlot v.13.0. As a result, a  
265 characteristic unit vector ( $\vec{P}$ ) was determined for each degradation pathway (see SI and  
266 Table S1). For a given degradation pathway, the unit vector  $\vec{P}$  can also be calculated from  
267  $\epsilon_{\text{bulk}}$  values determined in laboratory experiments according to the expression

268

269 
$$\vec{P} = \frac{1}{\sqrt{(\epsilon_{\text{bulk}}^{\text{Cl}})^2 + (\epsilon_{\text{bulk}}^{\text{C}})^2 + (\epsilon_{\text{bulk}}^{\text{H}})^2}} \cdot (\epsilon_{\text{bulk}}^{\text{Cl}}, \epsilon_{\text{bulk}}^{\text{C}}, \epsilon_{\text{bulk}}^{\text{H}}) \quad (3)$$

270

271 provided that absolute  $\epsilon_{\text{bulk}}$  values are used (see SI). A comparison of  $\vec{P}$ -vectors  
272 determined by principal component analysis with those calculated from eq. 3 is available in  
273 the SI (Table S2).

274

## 275 **RESULTS AND DISCUSSION**

### 276 **Hydrogen isotopes fractionation**

277 Aerobic biodegradation experiments lasted between 12 and 21 hours (half-life from ~3.5 to  
278 ~6.3 hours, see SI) and 1,2-DCA transformation above 90% was reached for all replicates.  
279  $\delta^2\text{H}$  values for 1,2-DCA showed a trend towards more positive values during its  
280 transformation by C-H bond oxidation (Figure 1a) or hydrolytic dehalogenation (Figure  
281 1b), reflecting an enrichment of 1,2-DCA in the heavy isotope ( $^2\text{H}$ ). This is indicative of a  
282 normal isotope effect. The  $\delta^2\text{H}$  values for 1,2-DCA in the controls remained constant  
283 throughout the experiments ( $\delta^2\text{H}_{\text{VSMOW-SLAP}} = -53 \pm 3\text{‰}$ ,  $\pm 1\sigma$ ,  $n = 6$ ). For *Pseudomonas* sp.  
284 strain DCA1 (C-H bond oxidation, Scheme 1a) a very large shift in  $\delta^2\text{H}$  values was  
285 observed, with up to  $\Delta\delta^2\text{H}_{\text{VSMOW-SLAP}} = +188 \pm 10\text{‰}$  after ~80% degradation (Figure 1a).  
286 This resulted in a large  $\epsilon_{\text{bulk}}^{\text{H}}$  value of  $-115 \pm 18\text{‰}$  ( $\text{AKIE}_{\text{H}} = 1.6 \pm 0.2$ ). Large  $\epsilon_{\text{bulk}}^{\text{H}}$  values  
287 were also observed, for instance, during oxidation of ethylbenzene by *Aromatoleum*  
288 *aromaticum* ( $\epsilon_{\text{bulk}}^{\text{H}} = -111 \pm 7\text{‰}$ ,  $\text{AKIE}_{\text{H}} = 6.0$ , for variations of  $\delta^2\text{H}$  within the range  $\Delta\delta^2\text{H}$   
289  $< 100$ )<sup>41</sup> or methyl *tert*-butyl ether (MTBE) by *Pseudonocardia tetrahydrofuranoxydans*  
290 K1 ( $\epsilon_{\text{bulk}}^{\text{H}} = -100 \pm 10\text{‰}$ ,  $\text{AKIE}_{\text{H}} = 14.2$ )<sup>42</sup>. In comparison to the large  $\epsilon_{\text{bulk}}^{\text{H}}$  value  
291 determined for oxidation of 1,2-DCA, for hydrolytic dehalogenation of 1,2-DCA (C-Cl  
292 bond cleavage via  $\text{S}_{\text{N}}2$ , Scheme 1b) a much lower enrichment in  $^2\text{H}$  was measured in  
293 experiments with *A. aquaticus* and *X. autotrophicus* ( $\epsilon_{\text{bulk}}^{\text{H}}$  values of  $-34 \pm 4\text{‰}$  and  $-38 \pm$   
294  $4\text{‰}$ , respectively, Figure 1b).

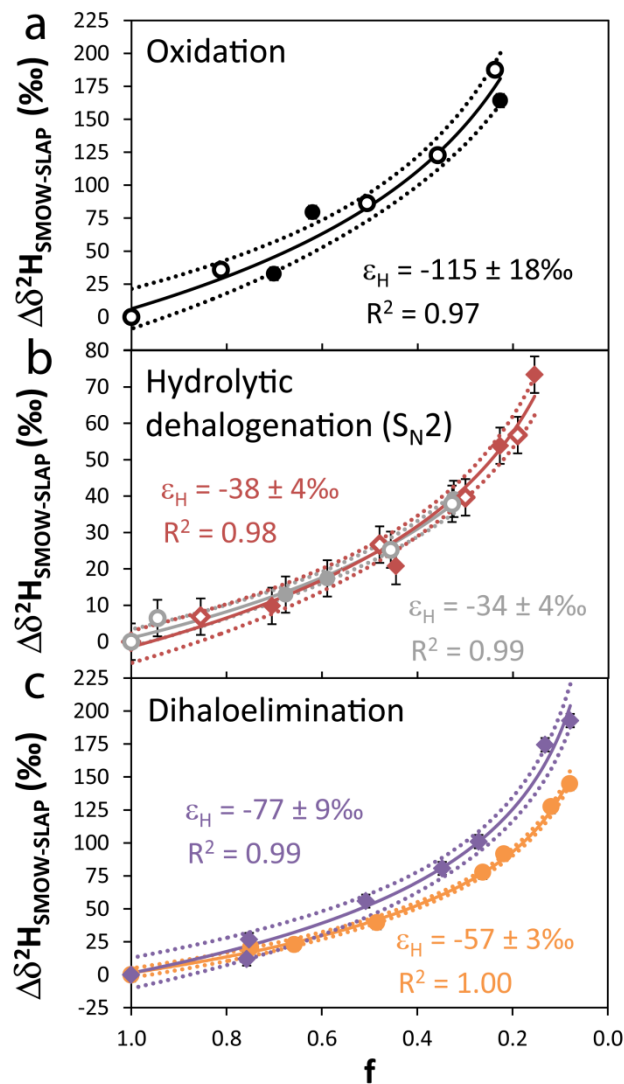
295 Anaerobic biodegradation experiments lasted approximately 9 and 40 days (half-life of ~30  
296 and ~289 hours, see SI) for the microcosms with *Dehalococcoides* and *Dehalogenimonas*-  
297 containing cultures, respectively, at which point most all of the initial 1,2-DCA was  
298 transformed to ethene via dihaloelimination. VC was detected only in the  
299 *Dehalococcoides*-containing microcosms, at concentrations much lower than those of  
300 ethene. The maximum accumulation of VC represented less than 6% of the initial 1,2-DCA  
301 added. Further information on concentrations of ethene and VC during degradation of 1,2-

302 DCA is available in a previous study.<sup>14</sup> The concentration pattern of products observed in  
303 this previous study<sup>14</sup> indicated that ethene and VC were formed in parallel reaction  
304 pathways via dihaloelimination and dehydrohalogenation (Scheme 1), respectively. Hence,  
305 products concentrations indicated that only a small fraction of 1,2-DCA was transformed  
306 via dehydrohalogenation in the *Dehalococcoides*-containing microcosms.

307 As observed for the aerobic experiments, enrichment in <sup>2</sup>H was obtained during  
308 dihaloelimination of 1,2-DCA by both anaerobic enrichment cultures ( $\epsilon_{\text{bulk}}^{\text{H}}$  values of  $-57 \pm$   
309  $3\text{‰}$  and  $-77 \pm 9\text{‰}$ , Figure 1c). However, in contrast to the similar  $\epsilon_{\text{bulk}}^{\text{H}}$  values obtained for  
310 hydrolytic dehalogenation by *A. aquaticus* and *X. autotrophicus*, a significantly higher  
311 value was determined for dihaloelimination by *Dehalogenimonas* ( $\epsilon_{\text{bulk}}^{\text{H}} = -77 \pm 9\text{‰}$ )  
312 compared to that of *Dehalococcoides* ( $\epsilon_{\text{bulk}}^{\text{H}} = -57 \pm 3\text{‰}$ ) containing cultures. The  $\delta^2\text{H}$   
313 values for 1,2-DCA in the controls did not change significantly during both experiments  
314 (i.e.,  $\delta^2\text{H}_{\text{VSMOW-SLAP}}$  of  $-44 \pm 1\text{‰}$  and  $-50 \pm 2\text{‰}$ ,  $\pm 1\sigma$ ,  $n = 4$ , respectively). It is also  
315 interesting to note that, although 1,2-DCA was purchased from different suppliers in each  
316 laboratory (see SI), their hydrogen isotopic signatures were relatively similar, varying  
317 between  $\delta^2\text{H}_{\text{VSMOW-SLAP}}$  values of  $-44 \pm 1\text{‰}$  and  $-53 \pm 3\text{‰}$ .

318 Even though clearly distinct  $\epsilon_{\text{bulk}}^{\text{H}}$  values were determined for different aerobic and  
319 anaerobic biodegradation pathways for 1,2-DCA during experiments performed in the  
320 laboratory, pathway distinction based on isotope fractionation of one element alone is not  
321 possible under field conditions. The reason is that changes in substrate concentrations are  
322 also related to processes other than transformation (e.g., hydrodynamic dispersion). This  
323 prevents accurate calculation of  $\epsilon_{\text{bulk}}^{\text{H}}$  values and, hence, precludes mechanistic information  
324 based on isotope effects. The situation is different if isotope analysis is conducted on two  
325 or more elements. The proportion of changes in  $\delta$ -values of both elements relative to each  
326 other (e.g.,  $\Delta\delta^2\text{H} / \Delta\delta^{13}\text{C}$ ) is largely unaffected by non-degradative processes.<sup>43, 44</sup>

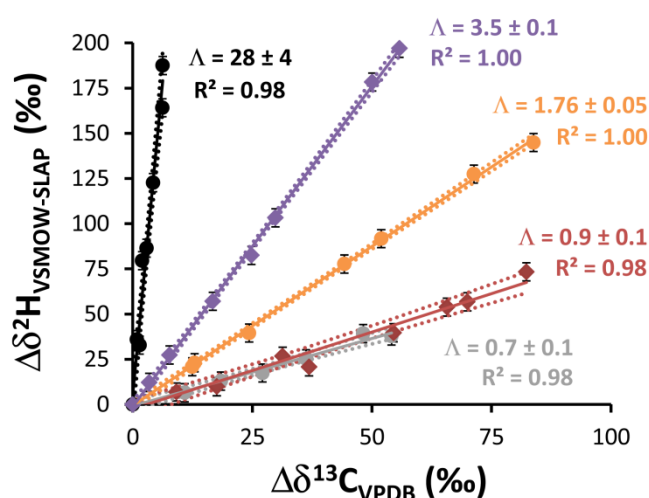
327 Therefore, measurements of isotope fractionation of two or more elements are crucial for  
 328 investigating contaminant biodegradation pathways in the field.



329  
 330 **Figure 1.** Hydrogen isotopic fractionation of 1,2-DCA during biodegradation by  
 331 *Pseudomonas* sp. (a), *A. aquaticus* (b, grey circles), *X. autotrophicus* (b, red diamonds) and  
 332 *Dehalococcoides*- (c, orange circles) and *Dehalogenimonas*-containing cultures (c, violet  
 333 diamonds); f is the fraction of 1,2-DCA remaining. For the aerobic experiments (a, b),  
 334 solid and empty symbols represent data from two replicate bottles. The error bars for  
 335 isotope values in panels (a) and (c) are smaller than the symbols. The solid lines are fits in  
 336 SigmaPlot<sup>®</sup> according to eq. 2 and dotted lines the 95% confidence intervals of the  
 337 nonlinear regressions.

### 338 Multi-element isotope approach

339 Hydrogen  $\delta$ -values of 1,2-DCA were combined with previously determined carbon and  
340 chlorine isotopic data for these experiments<sup>14, 24</sup> in dual- ( $\delta^2\text{H}$  vs.  $\delta^{13}\text{C}$  and  $\delta^2\text{H}$  vs.  $\delta^{37}\text{Cl}$ )  
341 and multi-element ( $\delta^2\text{H}$  vs.  $\delta^{13}\text{C}$  vs.  $\delta^{37}\text{Cl}$ ) isotope plots. The dual C-H isotope approach  
342 resulted in very good linear correlations ( $r^2 \geq 0.98$ , Figure 2), which is consistent with  
343 Dorer *et al.*<sup>41</sup> These authors showed that for variations of  $\delta^2\text{H}$  within the range  $\Delta\delta^2\text{H} < 100$   
344 – 200‰, the  $\epsilon_{\text{bulk}}^{\text{H}}$  and  $\Lambda_{\text{C-H}}$  values (i.e.,  $\Lambda_{\text{C-H}} = \Delta\delta^2\text{H} / \Delta\delta^{13}\text{C} \approx \epsilon_{\text{bulk}}^{\text{H}} / \epsilon_{\text{bulk}}^{\text{C}}$ ) can be  
345 evaluated using eq. 2 (Figure S1) and  $\Delta\delta^2\text{H}$  against  $\Delta\delta^{13}\text{C}$  data in a dual element isotope  
346 plot (Figure 2), respectively. A different procedure may be necessary for evaluating  
347 stronger H isotope fractionation that lead to larger shifts in  $\delta^2\text{H}$ , since previous studies  
348 observed a nonlinear behavior in H isotope ratios in Rayleigh and dual element isotope  
349 plots at a late stage of reaction.<sup>38, 41</sup>



350  
351 **Figure 2.** Dual C-H isotope trends during biodegradation of 1,2-DCA via oxidation by  
352 *Pseudomonas* sp. (black circles), hydrolytic dehalogenation by *A. aquaticus* (grey circles)  
353 and *X. autotrophicus* (red diamonds), and dihaloelimination by *Dehalococcoides*- (orange  
354 circles) and *Dehalogenimonas*-containing cultures (violet diamonds). Dotted lines indicate  
355 the 95% confidence intervals of the linear regression. Error bars of  $\Delta\delta^{13}\text{C}$  values are

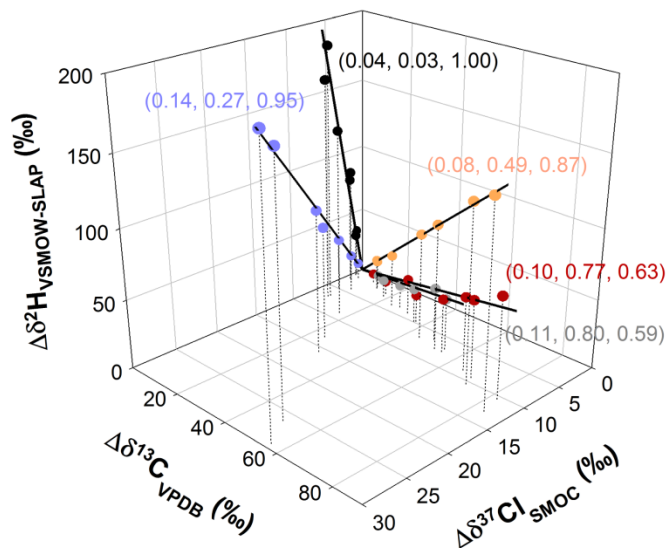
356 smaller than the symbols.  $\Lambda$  values ( $\pm 95\%$  C.I.) are given by the slope of the linear  
357 regressions.

358 The clearly distinct isotope patterns observed in Figure 2 for all the investigated  
359 degradation pathways, with  $\Lambda_{C-H}$  values ranging between  $28 \pm 4$  (oxidation) and  $0.8 \pm 0.1$   
360 (average value for hydrolytic dehalogenation), opens the possibility of a dual C-H isotope  
361 approach to identify the different aerobic and anaerobic degradation pathways for 1,2-DCA  
362 in the field. Particularly, for aerobic hydrolytic dehalogenation by *X. autotrophicus* and *A.*  
363 *aquaticus* (average  $\Lambda_{C-H}$  value of  $0.8 \pm 0.1$ ) and reductive dihaloelimination by a  
364 *Dehalococcoides*-containing culture ( $\Lambda_{C-H} = 1.76 \pm 0.05$ ), a larger relative difference in  
365  $\Lambda_{C-H}$  values was obtained (around 50% relative to the higher value) compared to that of  
366 their respective  $\Lambda_{C-Cl}$  values (around 10%, Scheme 1). Therefore, the use of a C-H isotope  
367 approach enables improved identification of the two pathways (i.e., hydrolytic  
368 dehalogenation and dihaloelimination).

369 A dual Cl-H isotope approach was also investigated and good linear correlations ( $r^2 \geq$   
370 0.97, Figure S2) were observed for all the degradation experiments in a dual isotope plot  
371 (see SI). However, similar  $\Lambda_{Cl-H}$  values were obtained for aerobic hydrolytic  
372 dehalogenation by *X. autotrophicus* and *A. aquaticus* ( $6.5 \pm 1.0$  and  $5.7 \pm 0.9$ , respectively)  
373 and dihaloelimination by a *Dehalogenimonas*-containing culture ( $6.7 \pm 0.3$ ), which  
374 hampers differentiation of these two pathways (i.e., hydrolytic dehalogenation and  
375 dihaloelimination) using a dual Cl-H isotope approach.

376 The large differences among all trends obtained for the dual C-H isotope approach  
377 (Figure 2) also enables estimation of the proportion of two competing pathways (e.g.,  
378 oxidation and hydrolytic dehalogenation reactions under aerobic conditions or  
379 dihaloelimination by *Dehalococcoides* and *Dehalogenimonas* populations under anaerobic  
380 conditions) based on the resultant slope,<sup>45, 46</sup> assuming simultaneous activity with a

381 constant ratio between both pathway rates. However, for three or more pathways unique  
382 solutions are not possible. An improved evaluation of up to three different degradation  
383 pathways might be possible by combining isotope data of three elements.



384  
385 **Figure 3.** Multi-element isotope patterns during biodegradation of 1,2-DCA via different  
386 reaction pathways: oxidation by *Pseudomonas* sp. (black), hydrolytic dehalogenation by *A.*  
387 *aquaticus* (grey) and *X. autotrophicus* (red), and dihaloelimination by *Dehalococcoides*-  
388 (orange) and *Dehalogenimonas*-containing cultures (violet). Solid lines are defined by the  
389 unit  $\vec{P}$ -vectors indicated in brackets (Table S1).

390 Measurement of hydrogen isotope ratios enables the combination of  $\delta^2\text{H}$  with  $\delta^{13}\text{C}$  and  
391  $\delta^{37}\text{Cl}$  data in a multi-element isotope plot (Figure 3). This new approach was investigated  
392 to determine whether the multi-element isotope patterns are sufficiently different to  
393 potentially distinguish among different aerobic and anaerobic biodegradation pathways in  
394 the field. As observed in Figure 3, the strongly different trends further strengthen pathway  
395 identification in future biodegradation studies for 1,2-DCA. In order to identify the  
396 degradation pathway of 1,2-DCA using a 3D approach, multi-element isotope data from  
397 new field (or laboratory) studies can be characterized by principal component analysis (see  
398 SI). The obtained  $\vec{P}$ -vector can then be compared to those reference  $\vec{P}$ -vectors reported in

399 this study for different reactions (Figure 3) by determining the angle between them (see  
400 S.I., eq S8). In complex sites where different biodegradation pathways may be involved,  
401 the occurrence of up to three different pathways might be detected using a 3D approach.  
402 For instance, in a site where three potential biodegradation pathways may control the fate  
403 of 1,2-DCA (e.g., aerobic biodegradation via oxidation and hydrolytic dehalogenation and  
404 anaerobic dihaloelimination by *Dehalogenimonas* populations), data points situated  
405 between their respective reference  $\vec{P}$ -vectors would indicate the effect of all of them.  
406 However, unequivocal information is hampered if more than three pathways occur at the  
407 site. If there are more than three pathways, additional information (e.g., redox data) is  
408 required to constrain pathways.

409 The distinctly different  $\Lambda_{C-H}$  values in Figure 2 can be rationalized in terms of the  
410 corresponding degradation mechanisms. For oxidation of 1,2-DCA, a highly pronounced H  
411 isotope fractionation was observed ( $\epsilon_{\text{bulk}}^{\text{H}} = -115 \pm 18\%$ ), reflecting a strong primary H  
412 isotope effect during oxidative C-H bond cleavage (Scheme 1a). In addition, smaller but  
413 non-negligible secondary isotope effects in H atoms located in proximity to the reacting  
414 bond (see below) are likely represented in the observable bulk fractionation.<sup>41, 47</sup> In  
415 contrast, for hydrolytic dehalogenation and dihaloelimination reactions (Schemes 1b-d),  
416 smaller  $\epsilon_{\text{bulk}}^{\text{H}}$  values were determined, ranging from  $-34 \pm 4\%$  to  $-77 \pm 9\%$ , since only  
417 secondary H isotope effects are involved during C-Cl bond cleavage. Conversely, a lower  
418  $\epsilon_{\text{bulk}}^{\text{C}}$  value was obtained for carbon during oxidation ( $-3.5 \pm 0.1\%$  for C-H bond  
419 cleavage),<sup>24</sup> relative to those determined for hydrolytic dehalogenation and  
420 dihaloelimination reactions (from  $-23 \pm 2\%$  to  $-33.0 \pm 0.4\%$  for C-Cl bond cleavage),<sup>14, 24</sup>  
421 due to the different mass of its bonding partner.<sup>34</sup> As a result, the largest  $\Lambda_{C-H}$  value was  
422 obtained for the C-H oxidation pathway (Figure 2). For the reactions without an initial  
423 primary H isotope effect, the different  $\epsilon_{\text{bulk}}^{\text{H}}$  values for hydrolytic dehalogenation (average

424 value of  $-36 \pm 3\text{‰}$ ) and dihaloelimination by *Dehalococcoides* ( $-57 \pm 3\text{‰}$ ) and  
425 *Dehalogenimonas* ( $-77 \pm 9\text{‰}$ ) containing cultures compared with their relatively similar  
426  $\epsilon_{\text{bulk}}^{\text{C}}$  values (from  $-23 \pm 2\text{‰}$  to  $-33.0 \pm 0.4\text{‰}$ )<sup>14, 24</sup> also resulted in distinctly different  $\Delta_{\text{C-H}}$   
427 values (Figure 2). The variation between  $\epsilon_{\text{bulk}}^{\text{H}}$  values for hydrolytic dehalogenation and  
428 dihaloelimination reactions and also between dihaloelimination by *Dehalococcoides* and  
429 *Dehalogenimonas*-containing cultures is discussed below.

### 430 **Secondary H isotope fractionation and insight into anaerobic dihaloelimination** 431 **mechanism**

432 During transformation of 1,2-DCA by *A. aquaticus* and *X. autotrophicus* by a haloalkane  
433 hydrolytic dehalogenase reaction (i.e., nucleophilic substitution S<sub>N</sub>2-type,<sup>5, 6</sup> Scheme 1b), a  
434 single C-Cl bond cleavage occurs in the first reaction step. Therefore, no primary H isotope  
435 effect would be expected for this pathway and the measured  $\epsilon_{\text{bulk}}^{\text{H}}$  values ( $-34 \pm 4\text{‰}$  and -  
436  $38 \pm 4\text{‰}$ ) represent the average secondary H isotope fractionation of all positions, i.e.,  $\alpha$ -  
437 secondary isotope effects in two H atoms located next to the reacting bond and  $\beta$ -  
438 secondary isotope effects in two H atoms situated one position away from the reacting  
439 bond. The H atoms situated one bond apart from the reacting bond might exhibit a smaller  
440 secondary isotope effect (see<sup>33, 34</sup> and references herein) compared to those atoms adjacent  
441 to the reaction bond. For instance,  $\alpha$ -secondary KIE<sub>H</sub> = 1.1-1.2 and  $\beta$ -secondary KIE<sub>H</sub> =  
442 1.05-1.15 are expected for a nucleophilic substitution S<sub>N</sub>1-type involving C-Cl bonds.<sup>34</sup>

443 Similarly to hydrolytic dehalogenation, no primary H isotope effect is expected in the  
444 initial transformation of 1,2-DCA by *Dehalococcoides* and *Dehalogenimonas*-containing  
445 cultures since no C-H bond is broken during dihaloelimination of 1,2-DCA to ethene  
446 (Scheme 1c). However, much higher secondary  $\epsilon_{\text{bulk}}^{\text{H}}$  values ( $-57 \pm 3\text{‰}$  and  $-77 \pm 9\text{‰}$ )  
447 were determined for both cultures compared to those obtained for hydrolytic  
448 dehalogenation. The large secondary compound average H isotope fractionation values

449 measured for dihaloelimination are  $\sim 50 - 70\%$  of that measured for C-H oxidation by  
450 *Pseudomonas* ( $-115 \pm 18\%$ ), which is remarkable given that no C-H bond is broken in the  
451 dihaloelimination reaction.

452 For enzymatic dihaloelimination of 1,2-DCA, a previous study based on C and Cl  
453 isotope fractionation suggested that the difference between  $\epsilon_{\text{bulk}}^{\text{C}}$  and  $\epsilon_{\text{bulk}}^{\text{Cl}}$  values obtained  
454 in experiments with *Dehalococcoides* and *Dehalogenimonas*-containing cultures could be  
455 associated with a different mode of *concerted* bond cleavage rather than with *stepwise*  
456 versus *concerted* reactions (Scheme 1c, d).<sup>14</sup> Assuming *concerted* dihaloelimination of 1,2-  
457 DCA (Scheme 1c),  $\alpha$ -secondary isotope effects may be anticipated for all H atoms. The  
458 location of all H atoms next to simultaneously reacting bonds could explain the higher  
459 secondary  $\epsilon_{\text{bulk}}^{\text{H}}$  values measured for dihaloelimination compared to hydrolytic  
460 dehalogenation, where  $\beta$ -secondary isotope effects are involved in the latter.

461  $\alpha$ -secondary AKIEs of  $1.060 \pm 0.003$  and  $1.08 \pm 0.01$  were calculated for *concerted*  
462 dihaloelimination of 1,2-DCA by *Dehalococcoides* and *Dehalogenimonas*-containing  
463 cultures, respectively, assuming simultaneous secondary effects without intramolecular  
464 competition (see SI). These values agree well with the  $\alpha$ -secondary KIE<sub>H</sub> (i.e., from 0.95 to  
465 1.2) reported for nucleophilic substitution ( $\text{S}_{\text{N}}1$ - and  $\text{S}_{\text{N}}2$ -type).<sup>34</sup> The different magnitude  
466 of  $\alpha$ -secondary AKIE<sub>H</sub> during 1,2-DCA transformation by *Dehalococcoides* and  
467 *Dehalogenimonas*-containing cultures might reflect a different interaction mode between  
468 reductive dehalogenases and 1,2-DCA (e.g., how leaving groups were stabilized in  
469 different enzyme environments) as previously proposed to explain the differences on C and  
470 Cl isotope effects (see Palau *et al.*<sup>14</sup> and references therein). Comparison of the hydrogen  
471 AKIEs determined in this study with those obtained using quantum mechanical/molecular  
472 mechanical modeling (QM/MM) in future studies can help to elucidate the enzymatic  
473 reaction mechanisms in more detail.

474 The evidence from H isotope ratios obtained in this study are in agreement with  
475 *concerted* dihaloelimination of 1,2-DCA by *Dehalococcoides* and *Dehalogenimonas*-  
476 containing cultures, showing that further insight into enzymatic reductive dechlorination of  
477 1,2-DCA can be obtained from hydrogen isotope fractionation. Such insight cannot be  
478 obtained from end product analysis because the same product (i.e., ethene) is formed  
479 during transformation of 1,2-DCA via *concerted* or *stepwise* dihaloelimination (Scheme  
480 1c,d). As observed for 1,2-DCA in this study, the different magnitude of secondary H  
481 isotope effects might help to differentiate between *concerted* and *stepwise*  
482 dihaloelimination mechanisms during biodegradation of other chlorinated ethanes of  
483 environmental concern, such 1,1,2-trichloroethane or 1,1,2,2-tetrachloroethane, in future  
484 studies.

#### 485 **Environmental Significance**

486 In addition to elucidating natural biodegradation processes for 1,2-DCA, multi-element  
487 isotope analysis can also be useful for obtaining insight into enhanced remediation  
488 processes such as in-situ bioaugmentation.<sup>48-50</sup> This form of enhanced biodegradation  
489 typically reduces the time required to reach target remediation goals at contaminated sites.  
490 However, its application and evaluation can be difficult at numerous sites impacted by  
491 mixtures of chlorinated compounds such as ethenes and ethanes. A recent study by Mayer-  
492 Blackwell *et al.*<sup>51</sup> showed that reductive dihaloelimination of 1,2-DCA by a  
493 *Dehalococcoides mccartyi* consortium was strongly inhibited by *cis*-DCE. These authors  
494 also suggested that the presence of a significant 1,2-DCA concentration in groundwater  
495 that is co-contaminated with chlorinated ethenes may alter the *Dehalococcoides* population  
496 structure away from conditions ideal for complete degradation of VC. In this case,  
497 degradation of 1,2-DCA by other ORB such as *Dehalogenimonas* could eventually  
498 eliminate its inhibitory effect on VC degradation by *Dehalococcoides* populations in the

499 field. Therefore, knowledge of the fate of 1,2-DCA at sites co-contaminated with  
500 chlorinated ethenes is crucial for site remediation. However, the assessment of 1,2-DCA  
501 transformation by *Dehalococcoides* or *Dehalogenimonas* populations in groundwater co-  
502 contaminated with chlorinated ethenes is particularly challenging because the same  
503 products (i.e., ethene and VC) are also obtained during biodegradation of chlorinated  
504 ethenes. The results of this study show that dihaloelimination of 1,2-DCA by ORB such  
505 *Dehalococcoides* or *Dehalogenimonas* could be identified using a dual- ( $\delta^2\text{H}$  vs.  $\delta^{13}\text{C}$ ) and  
506 a multi-element ( $\delta^2\text{H}$  vs.  $\delta^{13}\text{C}$  vs.  $\delta^{37}\text{Cl}$ ) isotope approach, illustrating the potential of H  
507 isotope analysis in combination with C and Cl isotope data to investigate transformation  
508 pathways for 1,2-DCA in the field. In addition to the ORBs investigated in this study, other  
509 anaerobic bacteria are also able to reductively dechlorinate 1,2-DCA. Therefore, the multi-  
510 element isotope patterns determined for the *Dehalococcoides* and *Dehalogenimonas*-  
511 containing enrichment cultures should be compared to the patterns obtained using other  
512 types of microbes, such *Dehalobacter*<sup>8</sup> or *Desulfitobacterium*,<sup>52</sup> in future studies.

513 Identification of the 1,2-DCA degradation pathway in the field can help constrain the  
514 range of  $\epsilon_{\text{bulk}}$  values used to estimate contaminant degradation extent using the Rayleigh  
515 equation,<sup>53, 54</sup> which is one of the main applications of CSIA to field studies. The new  
516 hydrogen isotope fractionation values for 1,2-DCA determined in this study, under both  
517 oxic and anoxic conditions, opens the possibility for using H-CSIA to quantify degradation  
518 at sites polluted by 1,2-DCA. In addition, the  $\epsilon_{\text{bulk}}^{\text{H}}$  values for the different reaction  
519 pathways determined in this study are larger than their respective  $\epsilon_{\text{bulk}}^{\text{C}}$ <sup>13, 14, 24, 35, 55-58</sup> and  
520  $\epsilon_{\text{bulk}}^{\text{Cl}}$ <sup>14, 24</sup> values, indicating that hydrogen isotopic fractionation can be a more sensitive  
521 indicator than carbon and chlorine isotopic fractionation. This can be particularly important  
522 for obtaining a better assessment of microbial oxidation of 1,2-DCA in the field ( $\epsilon_{\text{bulk}}^{\text{H}} = -$

523  $115 \pm 18\%$  compared to the  $\epsilon_{\text{bulk}}^{\text{C}}$  average value of  $-3.8 \pm 0.8\%$ ,  $\pm 1\sigma$ ,  $n = 6$ <sup>24, 57</sup> and the  
524  $\epsilon_{\text{bulk}}^{\text{Cl}}$  value of  $-3.8 \pm 0.2$ <sup>24</sup>).

525 Groundwater contaminant plumes are dynamic and highly heterogeneous systems  
526 subject to temporal and spatial geochemical variations that control biodegradation  
527 processes in an aquifer.<sup>59</sup> At contaminated sites, multi-isotope analysis in combination with  
528 appropriately high resolution sampling could be used to investigate the distribution of 1,2-  
529 DCA biodegradation processes associated with steep redox gradients, from oxic to anoxic  
530 environments (e.g., as often occurs with depth), which has rarely been considered in  
531 contaminant biodegradation studies. Understanding active degradation processes in the  
532 field is essential for evaluating natural attenuation and predicting how far a groundwater  
533 plume of 1,2-DCA might migrate. In this case, it is important to know if aerobic or  
534 anaerobic biodegradation occurs, especially since aerobic degradation rates for 1,2-DCA  
535 are likely controlled by the availability of oxygen. Hence, the conceptual model, and  
536 accordingly the mathematical model, used to predict plume behavior would be quite  
537 different. It also has implications for enhancing one remediation approach over another,  
538 e.g., adding more oxygen or adding electron donor, depending on the identified  
539 biodegradation pathway. Based on the results of this study, multi-element isotope patterns  
540 are expected i) to identify the active transformation pathway for 1,2-DCA; and ii) to detect  
541 changes in biodegradation conditions (i.e., aerobic vs. anaerobic biodegradation) allowing  
542 for better characterization of degradation processes in the field.

543 ASSOCIATED CONTENT

#### 544 **Supporting Information**

545 Further information about chemicals, analytical methods, reaction kinetics, correction of  
546 the substrate remaining fraction, Rayleigh isotope plot, calculation of H-AKIEs, dual Cl-H

547 isotope plot, and characterization of multi-element (Cl, C, H) isotope trends is available.

548 This material is available free of charge via the Internet at <http://pubs.acs.org>.

#### 549 AUTHOR INFORMATION

##### 550 **Corresponding Author\***

551 Jordi Palau

552 Institute of Environmental Assessment and Water Research (IDAEA-CSIC), Jordi Girona,

553 18-26, 08034 Barcelona, Spain.

554 E-mail: [jordi.palau@ub.edu](mailto:jordi.palau@ub.edu)

##### 555 **Author Contributions**

556 The manuscript was written through contributions of all authors. All authors have given  
557 approval to the final version of the manuscript.

#### 558 ACKNOWLEDGEMENTS

559 We thoroughly thank four anonymous reviewers and the editor for their helpful comments  
560 on the manuscript. We also want to thank Dr Raimon Tolosana-Delgado for his comments  
561 on data analysis. J.P. was supported by the University of Neuchâtel via direct university  
562 funding. E.M-U is supported by the Spanish Ministry of Economy and Competitiveness  
563 and FEDER (project CTM2013-48545-C2-1-R) and the Xarxa de Referència en  
564 Biotecnologia de la Generalitat de Catalunya. MAG group is supported by Spanish  
565 Government REMEDIATION project (CGL2014-57215-C4-1-R) and the Catalan  
566 Government project 2014SGR-1456. S.H.M acknowledges support from the Ministry of  
567 Education Malaysia (SLAI-UMP Scholarship) for a predoctoral fellowship and M.R. a  
568 Ramón y Cajal contract (RYC-2012-11920).

569 **REFERENCES**

- 570 1. ATSDR Toxicological Profile for 1,2-Dichloroethane.  
571 <http://www.atsdr.cdc.gov/toxfaqs/tfacts38.pdf> (accessed July 17, 2017).
- 572 2. (EPA), U. S. E. P. A. Releases of Chemicals in the 2015 TRI National Analysis.  
573 <https://www.epa.gov/trinationalanalysis/releases-chemicals-2015-tri-national-analysis> (March 14,  
574 2017).
- 575 3. USEPA Priority pollutants. <http://water.epa.gov/scitech/methods/cwa/pollutants.cfm>  
576 (January 7, 2015).
- 577 4. Hage, J. C.; Hartmans, S., Monooxygenase-mediated 1,2-dichloroethane degradation by  
578 *Pseudomonas* sp. strain DCA1. *Appl Environ Microbiol* **1999**, *65*, (6), 2466-70.
- 579 5. van den Wijngaard, A. J.; van der Kamp, K. W.; van der Ploeg, J.; Pries, F.; Kazemier, B.;  
580 Janssen, D. B., Degradation of 1,2-dichloroethane by *Ancylobacter aquaticus* and other facultative  
581 methylotrophs. *Appl Environ Microbiol* **1992**, *58*, (3), 976-83.
- 582 6. Janssen, D. B.; Scheper, A.; Dijkhuizen, L.; Witholt, B., Degradation of halogenated  
583 aliphatic compounds by *Xanthobacter autotrophicus* GJ10. *Appl Environ Microbiol* **1985**, *49*, (3),  
584 673-7.
- 585 7. Klecka, G. M.; Carpenter, C. L.; Gonsior, S. J., Biological transformations of 1,2-  
586 dichloroethane in subsurface soils and groundwater. *J Contam Hydrol* **1998**, *34*, (1-2), 139-154.
- 587 8. Grostern, A.; Edwards, E. A., Characterization of a *Dehalobacter* Coculture That  
588 Dechlorinates 1,2-Dichloroethane to Ethene and Identification of the Putative Reductive  
589 Dehalogenase Gene. *Appl Environ Microbiol* **2009**, *75*, (9), 2684-2693.
- 590 9. Egli, C.; Scholtz, R.; Cook, A. M.; Leisinger, T., Anaerobic dechlorination of  
591 tetrachloromethane and 1,2-dichloroethane to degradable products by pure cultures of  
592 *Desulfobacterium* sp. and *Methanobacterium* sp. *FEMS Microbiol Lett* **1987**, *43*, (3), 257-261.
- 593 10. Yu, R.; Peethambaram, H. S.; Falta, R. W.; Verce, M. F.; Henderson, J. K.; Bagwell, C. E.;  
594 Brigmon, R. L.; Freedman, D. L., Kinetics of 1,2-Dichloroethane and 1,2-Dibromoethane  
595 Biodegradation in Anaerobic Enrichment Cultures. *Appl Environ Microbiol* **2013**, *79*, (4), 1359-  
596 1367.
- 597 11. Holliger, C.; Schraa, G.; Stams, A. J. M.; Zehnder, A. J. B., Reductive dechlorination of 1,2-  
598 dichloroethane and chloroethane by cell suspensions of methanogenic bacteria. *Biodegradation*  
599 **1990**, *1*, (4), 253-261.
- 600 12. Maymo-Gatell, X.; Anguish, T.; Zinder, S. H., Reductive dechlorination of chlorinated  
601 ethenes and 1,2-dichloroethane by "Dehalococcoides ethenogenes" 195. *Appl Environ Microbiol*  
602 **1999**, *65*, (7), 3108-3113.

- 603 13. Schmidt, M.; Lege, S.; Nijenhuis, I., Comparison of 1,2-dichloroethane, dichloroethene and  
604 vinyl chloride carbon stable isotope fractionation during dechlorination by two Dehalococcoides  
605 strains. *Water Res* **2014**, *52*, 146-54.
- 606 14. Palau, J.; Yu, R.; Hatijah Mortan, S.; Shouakar-Stash, O.; Rosell, M.; Freedman, D. L.;  
607 Sbarbati, C.; Fiorenza, S.; Aravena, R.; Marco-Urrea, E.; Elsner, M.; Soler, A.; Hunkeler, D., Distinct  
608 Dual C-Cl Isotope Fractionation Patterns during Anaerobic Biodegradation of 1,2-Dichloroethane:  
609 Potential To Characterize Microbial Degradation in the Field. *Environ Sci Technol* **2017**, *51*, (5),  
610 2685-2694.
- 611 15. Gossett, J. M., Sustained aerobic oxidation of vinyl chloride at low oxygen concentrations.  
612 *Environ Sci Technol* **2010**, *44*, (4), 1405-11.
- 613 16. van der Zaan, B.; de Weert, J.; Rijnaarts, H.; de Vos, W. M.; Smidt, H.; Gerritse, J.,  
614 Degradation of 1,2-dichloroethane by microbial communities from river sediment at various redox  
615 conditions. *Water Res* **2009**, *43*, (13), 3207-16.
- 616 17. Dinglasan-Panlilio, M. J.; Dworatzek, S.; Mabury, S.; Edwards, E., Microbial oxidation of  
617 1,2-dichloroethane under anoxic conditions with nitrate as electron acceptor in mixed and pure  
618 cultures. *FEMS Microbiol Ecol* **2006**, *56*, (3), 355-64.
- 619 18. Hirschorn, S. K.; Dinglasan-Panlilio, M. J.; Edwards, E. A.; Lacrampe-Couloume, G.;  
620 Sherwood Lollar, B., Isotope analysis as a natural reaction probe to determine mechanisms of  
621 biodegradation of 1,2-dichloroethane. *Environ Microbiol* **2007**, *9*, (7), 1651-7.
- 622 19. Sun, B. L.; Griffin, B. M.; Ayala-del-Rio, H. L.; Hashsham, S. A.; Tiedje, J. M., Microbial  
623 dehalorespiration with 1,1,1-trichloroethane. *Science* **2002**, *298*, (5595), 1023-1025.
- 624 20. Badin, A.; Buttet, G.; Maillard, J.; Holliger, C.; Hunkeler, D., Multiple Dual C-Cl Isotope  
625 Patterns Associated with Reductive Dechlorination of Tetrachloroethene. *Environ Sci Technol*  
626 **2014**, *48*, (16), 9179-9186.
- 627 21. Abe, Y.; Aravena, R.; Zopfi, J.; Shouakar-Stash, O.; Cox, E.; Roberts, J. D.; Hunkeler, D.,  
628 Carbon and Chlorine Isotope Fractionation during Aerobic Oxidation and Reductive Dechlorination  
629 of Vinyl Chloride and cis-1,2-Dichloroethene. *Environ Sci Technol* **2009**, *43*, (1), 101-107.
- 630 22. Cretnik, S.; Thoreson, K. A.; Bernstein, A.; Ebert, K.; Buchner, D.; Laskov, C.; Haderlein, S.;  
631 Shouakar-Stash, O.; Kliegman, S.; McNeill, K.; Elsner, M., Reductive Dechlorination of TCE by  
632 Chemical Model Systems in Comparison to Dehalogenating Bacteria: Insights from Dual Element  
633 Isotope Analysis ( $^{13}\text{C}/^{12}\text{C}$ ,  $^{37}\text{Cl}/^{35}\text{Cl}$ ). *Environ Sci Technol* **2013**, *47*, (13), 6855-6863.
- 634 23. Renpenning, J.; Keller, S.; Cretnik, S.; Shouakar-Stash, O.; Elsner, M.; Schubert, T.;  
635 Nijenhuis, I., Combined C and Cl isotope effects indicate differences between corrinoids and  
636 enzyme (Sulfurospirillum multivorans PceA) in reductive dehalogenation of tetrachloroethene, but  
637 not trichloroethene. *Environ Sci Technol* **2014**, *48*, (20), 11837-45.
- 638 24. Palau, J.; Cretnik, S.; Shouakar-Stash, O.; Hoche, M.; Elsner, M.; Hunkeler, D., C and Cl  
639 Isotope Fractionation of 1,2-Dichloroethane Displays Unique  $\delta(^{13}\text{C})/\delta(^{37}\text{Cl})$  Patterns for

- 640 Pathway Identification and Reveals Surprising C-Cl Bond Involvement in Microbial Oxidation.  
641 *Environ Sci Technol* **2014**, *48*, (16), 9430-7.
- 642 25. Zwank, L. Assessment of the fate of organic groundwater contaminants using their  
643 isotopic signatures. Swiss Federal Institute of Technology (ETH), Zürich, Switzerland, 2004.
- 644 26. Shouakar-Stash, O.; Drimmie, R. J., Online methodology for determining compound-  
645 specific hydrogen stable isotope ratios of trichloroethene and 1,2-cis-dichloroethene by  
646 continuous-flow isotope ratio mass spectrometry. *Rapid Commun Mass Sp* **2013**, *27*, (12), 1335-  
647 1344.
- 648 27. Renpenning, J.; Kummel, S.; Hitzfeld, K. L.; Schimmelmann, A.; Gehre, M., Compound-  
649 specific hydrogen isotope analysis of heteroatom-bearing compounds via gas chromatography-  
650 chromium-based high-temperature conversion (Cr/HTC)-isotope ratio mass spectrometry. *Anal*  
651 *Chem* **2015**, *87*, (18), 9443-50.
- 652 28. Kuder, T.; Philp, P., Demonstration of compound-specific isotope analysis of hydrogen  
653 isotope ratios in chlorinated ethenes. *Environ Sci Technol* **2013**, *47*, (3), 1461-7.
- 654 29. Renpenning, J.; Schimmelmann, A.; Gehre, M., Compound-specific hydrogen isotope  
655 analysis of fluorine-, chlorine-, bromine- and iodine-bearing organics using gas chromatography-  
656 chromium-based high-temperature conversion (Cr/HTC) isotope ratio mass spectrometry. *Rapid*  
657 *Commun Mass Spectrom* **2017**, *31*, (13), 1095-1102.
- 658 30. Audi-Miro, C.; Cretnik, S.; Torrento, C.; Rosell, M.; Shouakar-Stash, O.; Otero, N.; Palau, J.;  
659 Elsner, M.; Soler, A., C, Cl and H compound-specific isotope analysis to assess natural versus Fe(0)  
660 barrier-induced degradation of chlorinated ethenes at a contaminated site. *J Hazard Mater* **2015**,  
661 *299*, 747-54.
- 662 31. Ivdra, N.; Fischer, A.; Herrero-Martin, S.; Giunta, T.; Bonifacie, M.; Richnow, H. H., Carbon,  
663 Hydrogen and Chlorine Stable Isotope Fingerprinting for Forensic Investigations of  
664 Hexachlorocyclohexanes. *Environ Sci Technol* **2017**, *51*, (1), 446-454.
- 665 32. Kuder, T.; van Breukelen, B. M.; Vanderford, M.; Philp, P., 3D-CSIA: carbon, chlorine, and  
666 hydrogen isotope fractionation in transformation of TCE to ethene by a Dehalococcoides culture.  
667 *Environ Sci Technol* **2013**, *47*, (17), 9668-77.
- 668 33. Elsner, M., Stable isotope fractionation to investigate natural transformation mechanisms  
669 of organic contaminants: principles, prospects and limitations. *J Environ Monitor* **2010**, *12*, (11),  
670 2005-2031.
- 671 34. Elsner, M.; Zwank, L.; Hunkeler, D.; Schwarzenbach, R. P., A new concept linking  
672 observable stable isotope fractionation to transformation pathways of organic pollutants. *Environ*  
673 *Sci Technol* **2005**, *39*, (18), 6896-6916.
- 674 35. Hunkeler, D.; Aravena, R., Evidence of substantial carbon isotope fractionation among  
675 substrate, inorganic carbon, and biomass during aerobic mineralization of 1, 2-dichloroethane by  
676 *Xanthobacter autotrophicus*. *Appl Environ Microbiol* **2000**, *66*, (11), 4870-6.

- 677 36. Martin-Gonzalez, L.; Hatijah Mortan, S.; Rosell, M.; Parlade, E.; Martinez-Alonso, M.; Gaju,  
678 N.; Caminal, G.; Adrian, L.; Marco-Urrea, E., Stable Carbon Isotope Fractionation During 1,2-  
679 Dichloropropane-to-Propene Transformation by an Enrichment Culture Containing  
680 Dehalogenimonas Strains and a dcpA Gene. *Environ Sci Technol* **2015**, *49*, (14), 8666-74.
- 681 37. Elsner, M.; Couloume, G. L.; Lollar, B. S., Freezing to preserve groundwater samples and  
682 improve headspace quantification limits of water-soluble organic contaminants for carbon isotope  
683 analysis. *Anal Chem* **2006**, *78*, (21), 7528-7534.
- 684 38. Wijker, R. S.; Adamczyk, P.; Bolotin, J.; Paneth, P.; Hofstetter, T. B., Isotopic analysis of  
685 oxidative pollutant degradation pathways exhibiting large H isotope fractionation. *Environ Sci*  
686 *Technol* **2013**, *47*, (23), 13459-68.
- 687 39. Buchner, D.; Jin, B.; Ebert, K.; Rolle, M.; Elsner, M.; Haderlein, S. B., Experimental  
688 Determination of Isotope Enrichment Factors - Bias from Mass Removal by Repetitive Sampling.  
689 *Environ Sci Technol* **2017**, *51*, (3), 1527-1536.
- 690 40. Scott, K. M.; Lu, X.; Cavanaugh, C. M.; Liu, J. S., Optimal methods for estimating kinetic  
691 isotope effects from different forms of the Rayleigh distillation equation. *Geochim Cosmochim Acta*  
692 **2004**, *68*, (3), 433-442.
- 693 41. Dorer, C.; Hohener, P.; Hedwig, N.; Richnow, H. H.; Vogt, C., Rayleigh-based concept to  
694 tackle strong hydrogen fractionation in dual isotope analysis-the example of ethylbenzene  
695 degradation by *Aromatoleum aromaticum*. *Environ Sci Technol* **2014**, *48*, (10), 5788-97.
- 696 42. McKelvie, J. R.; Hyman, M. R.; Elsner, M.; Smith, C.; Aslett, D. M.; Lacrampe-Couloume, G.;  
697 Lollar, B. S., Isotopic fractionation of methyl tert-butyl ether suggests different initial reaction  
698 mechanisms during aerobic biodegradation. *Environ Sci Technol* **2009**, *43*, (8), 2793-9.
- 699 43. Tobler, N. B.; Hofstetter, T. B.; Schwarzenbach, R. P., Carbon and Hydrogen Isotope  
700 Fractionation during Anaerobic Toluene Oxidation by *Geobacter metallireducens* with Different  
701 Fe(III) Phases as Terminal Electron Acceptors. *Environ Sci Technol* **2008**, *42*, (21), 7786-7792.
- 702 44. Thullner, M.; Fischer, A.; Richnow, H. H.; Wick, L. Y., Influence of mass transfer on stable  
703 isotope fractionation. *Appl Microbiol Biotechnol* **2013**, *97*, (2), 441-52.
- 704 45. Centler, F.; Hesse, F.; Thullner, M., Estimating pathway-specific contributions to  
705 biodegradation in aquifers based on dual isotope analysis: Theoretical analysis and reactive  
706 transport simulations. *J Contam Hydrol* **2013**, *152*, 97-116.
- 707 46. van Breukelen, B. M., Extending the Rayleigh equation to allow competing isotope  
708 fractionating pathways to improve quantification of biodegradation. *Environ Sci Technol* **2007**, *41*,  
709 (11), 4004-10.
- 710 47. Elsner, M.; McKelvie, J.; Couloume, G. L.; Lollar, B. S., Insight into methyl tert-butyl ether  
711 (MTBE) stable isotope Fractionation from abiotic reference experiments. *Environ Sci Technol* **2007**,  
712 *41*, (16), 5693-5700.

- 713 48. Ellis, D. E.; Lutz, E. J.; Odom, J. M.; Buchanan, R. J.; Bartlett, C. L.; Lee, M. D.; Harkness, M.  
714 R.; DeWeerd, K. A., Bioaugmentation for Accelerated In Situ Anaerobic Bioremediation. *Environ Sci*  
715 *Technol* **2000**, *34*, (11), 2254-2260.
- 716 49. Major, D. W.; McMaster, M. L.; Cox, E. E.; Edwards, E. A.; Dworatzek, S. M.; Hendrickson,  
717 E. R.; Starr, M. G.; Payne, J. A.; Buonamici, L. W., Field demonstration of successful  
718 bioaugmentation to achieve dechlorination of tetrachloroethene to ethene. *Environ Sci Technol*  
719 **2002**, *36*, (23), 5106-16.
- 720 50. Maes, A.; van Raemdonck, H.; Smith, K.; Ossieur, W.; Lebbe, L.; Verstraete, W., Transport  
721 and activity of *Desulfitobacterium dichloroeliminans* strain DCA1 during bioaugmentation of 1,2-  
722 DCA-contaminated groundwater. *Environ Sci Technol* **2006**, *40*, (17), 5544-5552.
- 723 51. Mayer-Blackwell, K.; Fincker, M.; Molenda, O.; Callahan, B.; Sewell, H.; Holmes, S.;  
724 Edwards, E. A.; Spormann, A. M., 1,2-Dichloroethane Exposure Alters the Population Structure,  
725 Metabolism, and Kinetics of a Trichloroethene-Dechlorinating *Dehalococcoides mccartyi*  
726 Consortium. *Environ Sci Technol* **2016**, *50*, (22), 12187-12196.
- 727 52. De Wildeman, S.; Diekert, G.; Van Langenhove, H.; Verstraete, W., Stereoselective  
728 microbial dehalorespiration with vicinal dichlorinated alkanes. *Appl Environ Microbiol* **2003**, *69*,  
729 (9), 5643-7.
- 730 53. Thullner, M.; Centler, F.; Richnow, H. H.; Fischer, A., Quantification of organic pollutant  
731 degradation in contaminated aquifers using compound specific stable isotope analysis - Review of  
732 recent developments. *Org Geochem* **2012**, *42*, (12), 1440-1460.
- 733 54. Aelion, C. M.; Hohöner, P.; Hunkeler, D.; Aravena, R., *Environmental isotopes in*  
734 *biodegradation and bioremediation*. CRC Press: Boca Raton, 2010; p xiv, 450 p.
- 735 55. Hunkeler, D.; Aravena, R.; Cox, E., Carbon isotopes as a tool to evaluate the origin and fate  
736 of vinyl chloride: laboratory experiments and modeling of isotope evolution. *Environ Sci Technol*  
737 **2002**, *36*, (15), 3378-84.
- 738 56. Hirschorn, S. K.; Grostern, A.; Lacrampe-Couloume, G.; Edwards, E. A.; Mackinnon, L.;  
739 Repta, C.; Major, D. W.; Sherwood Lollar, B., Quantification of biotransformation of chlorinated  
740 hydrocarbons in a biostimulation study: added value via stable carbon isotope analysis. *J Contam*  
741 *Hydrol* **2007**, *94*, (3-4), 249-60.
- 742 57. Hirschorn, S. K.; Dinglasan, M. J.; Elsner, M.; Mancini, S. A.; Lacrampe-Couloume, G.;  
743 Edwards, E. A.; Lollar, B. S., Pathway dependent isotopic fractionation during aerobic  
744 biodegradation of 1,2-dichloroethane. *Environ Sci Technol* **2004**, *38*, (18), 4775-4781.
- 745 58. Abe, Y.; Zopfi, J.; Hunkeler, D., Effect of molecule size on carbon isotope fractionation  
746 during biodegradation of chlorinated alkanes by *Xanthobacter autotrophicus* GJ10. *Isotopes*  
747 *Environ Health Stud* **2009**, *45*, (1), 18-26.
- 748 59. Meckenstock, R. U.; Elsner, M.; Griebler, C.; Lueders, T.; Stumpp, C.; Aamand, J.; Agathos,  
749 S. N.; Albrechtsen, H. J.; Bastiaens, L.; Bjerg, P. L.; Boon, N.; Dejonghe, W.; Huang, W. E.; Schmidt,

750 S. I.; Smolders, E.; Sorensen, S. R.; Springael, D.; van Breukelen, B. M., Biodegradation: Updating  
751 the concepts of control for microbial cleanup in contaminated aquifers. *Environ Sci Technol* **2015**,  
752 *49*, (12), 7073-81.